IL NUOVO CIMENTO Vol. 34 C, N. 5 Settembre-Ottobre 2011
DOI 10.1393/ncc/i2011-10977-7

Communications: SIF Congress 2010

Geant4 simulation of a scintillator-lead shashlik calorimeter with a SiPM readout

A. Berra(*)

Università degli Studi dell'Insubria - Como, Italy
INFN, Sezione di Milano Bicocca - Milano, Italy

(ricevuto il 27 Dicembre 2010; revisionato il 24 Gennaio 2011; approvato il 24 Gennaio 2011; pubblicato online il 22 Settembre 2011)

Summary. — Shashlik calorimeters are sampling calorimeters which, in the last 20 years, have been used in many high-energy experiments: relatively cheap, they can be easily segmented and built in a large variety of geometries and they guarantee energy resolutions comparable to the ones achievable with homogeneous calorimeters. This article presents the complete optical simulation of a prototype of a scintillator-lead shashlik calorimeter with silicon photomultipliers readout, characterized in terms of linearity, energy and spatial resolution. The simulation has been used to explain and validate the experimental data, obtained on the PS-T9 beamline at CERN, using electrons in the 1–7 GeV energy range.

PACS 29.40.Mc – Scintillation detectors.
PACS 29.40.Vj – Calorimeters.
PACS 78.20.Bh – Theory, models, and numerical simulation.
PACS 29.40.Wk – Solid-state detectors.

In the last 50 years, sampling calorimeters have become the most used type of calorimeters in high-energy experiments. The main advantages of this type of detectors can be listed as follows:

– they can be built using various types of passive radiators (*i.e.* lead, tungsten, copper, iron and many other materials) and active sampling materials (plastic and liquid scintillator, gaseous materials and even silicon detectors);

– the passive and active materials can be tuned in terms of ratio and thickness to fulfill different physics requirements;

– they are simple to produce and relatively cheap compared to the homogeneous calorimeters.

(*) E-mail: alessandro.berra@gmail.com

© Società Italiana di Fisica

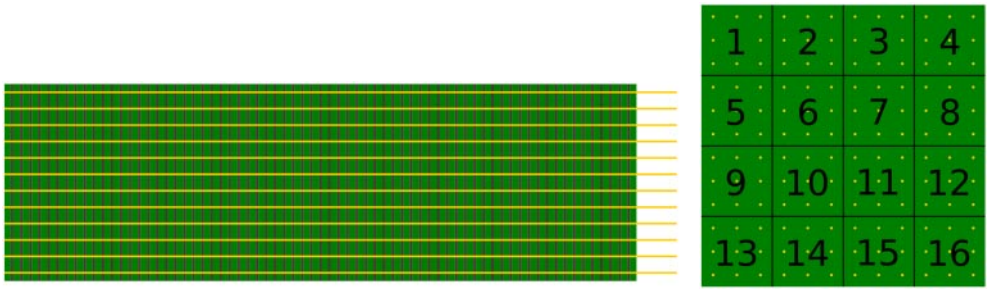

(a) (b)

Fig. 1. – Lateral (a) and frontal (b) sketch of the calorimeter; the numbers of the readout channels are also indicated.

Shashlik calorimeters are a particular type of sampling calorimeters in which the layers are crossed, for all their length, by wavelength shifter (WLS) fibers, which collect the scintillation light. The design of this type of calorimeter was proposed in 1985 by Fessler [1] and since then it has been used in many high-energy experiments, like in the electromagnetic calorimeter of the LHCb [2] detector or in the STIC luminometer [3] developed for the DELPHI [4] experiment. These detectors typically use organic/plastic scintillator as active material, thus reducing their costs, can be built in a large variety of geometries and can achieve a very good performance in terms of energy resolution as shown in [5].

Considering the high granularity, WLS readout in the longitudinal direction, a multichannel readout system such as a multianode photomultiplier [2] (PMT) or many silicon-based photo-detectors [6] can be used to measure with a certain accuracy the position of the shower inside the calorimeter. Among these devices, a new and very promising photosensitive silicon detector, called silicon photomultiplier (SiPM), has been proposed [7]. The advantages of these devices are the low operating voltage ($\sim 50\,\mathrm{V}$) with respect to photomultipliers, the high gain ($\sim 10^6$) and the insensitivity to magnetic fields.

This article describes the Monte Carlo simulation of a shashlik calorimeter with a SiPM readout performed with the Geant4 [8] toolkit and its beam tests. The first two sections of the article describe the shashlik calorimeter and its complete Geant4 simulation, considering also the propagation of the optical photons inside the device. The third section is devoted to the description of the experimental setup on the PS-T9 beamline at CERN and in the last section the comparison between simulated and real data is summarized.

1. – The scintillator-lead shashlik calorimeter

The shashlik calorimeter under test, built by the mechanical workshop of INFN-Trieste, is composed of 70 4 mm thick tiles of plastic scintillator and 69 1.5 mm thick tiles of lead, for a total of ~ 19 radiation lengths and a Molière radius of $\sim 6\,\mathrm{cm}$. Each tile has an area of $11.5 \times 11.5\,\mathrm{cm}^2$; the readout is performed using 144 1.2 mm WLS fibers (Saint-Gobain BCF-92 [9]). The sensitive part of the calorimeter is contained in a 1 cm thick aluminium vessel which covers the top and bottom parts of the tiles and guarantees the mechanical stability; no reflective material has been used at the interface between the scintillator and lead tiles to improve the light collection: this detail will be better discussed in sect. **2**. A sketch of the calorimeter is shown in fig. 1.

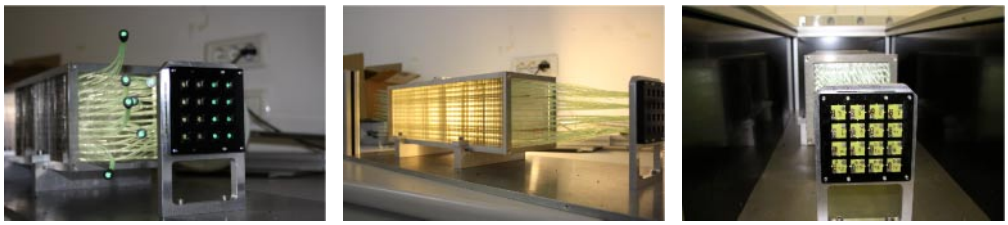

(a) (b) (c)

Fig. 2. – The calorimeter during the assembly phase: (a) fibers insertion; (b) the fibers plugged into the SiPM plastic holder; (c) the SiPMs placed into the holder.

The WLS fibers cross the whole calorimeter, so that each fiber collects the light of all the scintillator tiles. According to fig. 1(a) and (b), the fibers are placed in a 1 cm spaced 12×12 matrix of holes made in the scintillator and lead tiles; they are then grouped and glued in bundles of nine fibers each using 16 plastic holders, and plugged into a support designed to hold an array of SiPMs. A few pictures of the calorimeter during the assembly phases are presented in fig. 2.

2. – The Geant4 simulation

The calorimeter has been simulated in different ways using the Geant4 toolkit in order to characterize it in terms of linearity, energy and spatial resolutions. The first simulation has been performed generating a monochromatic beam of electrons in the 1–7 GeV energy range; the beam has been generated with a Gaussian shape with $\sigma = 1.5$ cm in both the horizontal and vertical directions. This simulation takes into account only the energy deposit of the electrons inside the scintillator tiles, without including the optical processes and the noise of the readout chain. The electromagnetic and hadronic interactions are taken into account using the QGSP_BERT physics list [10], a composite model which uses the Quark Gluon String and the Precompound model to parametrize the interactions above 10 GeV and the Bertini cascade model for the interactions below 10 GeV; this model handles also the electromagnetic interactions using the standard G4EmStandardPhysics list: the electromagnetic cuts on secondary particles have been set to 100 μm; these cuts are then converted in different energy cuts for each material by the Geant4 tracking kernel.

In order to define the energy linearity and resolution, the plot of the energy deposit in the scintillator tiles has been fitted with a Gaussian function: the resolution parameter has been defined as the sigma/mean ratio. The resolution energy scan has been fitted using the function $\frac{\sigma_E}{E} = P_0 \oplus \frac{P_1}{\sqrt{E}}$, where the $\oplus$ indicates that the terms are added in quadrature. In this function P_0 represents the constant term, which parametrizes the detector non-uniformities and imperfections and dominates at high energies, and P_1 represents the stochastic term which depends on the fluctuations related to the physical development of the shower [11]. The results obtained in terms of linearity and energy resolution are shown in fig. 3; here and in the following, the uncertainty bars on the linearity plots are the fitted mean parameter errors of the Gaussian distribution.

The simulation shows a very good linearity, a stochastic term of 7.0% and a constant term of the order of 1%. However, this simulation can be considered only as a best estimate of the calorimeter capabilities: inefficiencies due to the optical propagation of

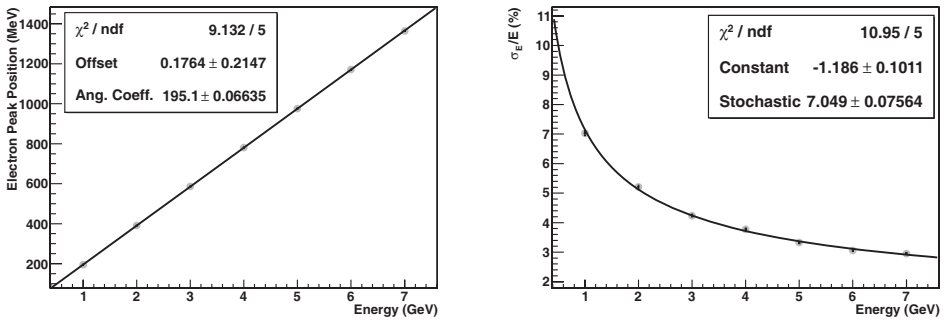

(a) (b)

Fig. 3. – Calorimeter linearity (a) and energy resolution (b) for seven monochromatic electron beams.

light inside the calorimeter or to the noise introduced by the readout chain can worsen the energy resolution. For these reasons a new Geant4 simulation has been developed with the purpose to study the inefficiencies that can be induced by the optical processes. This is obtained activating the *OpticalPhysics* physics list which handles a great number of optical processes, for example:

– reflection and refraction processes between materials with different refractive index;

– scintillation processes, handled in terms of yield and slow or fast emission components;

– Cherenkov light emission;

– exponential light attenuation inside the dielectric materials;

– wavelength shifting processes handled in terms of absorption and emission coefficients and characteristic time scales.

The drawback of this type of simulation is that each optical photon is tracked as a single particle: considering the large number of photons involved in the scintillation processes, the simulation requires a lot of CPU time ($\sim$ 9 minutes for each event with a 1 GeV electron beam).

The first step is the assignment of the optical properties to the materials which compose the calorimeter as the refractive index or the scintillation yield factor. The used values are extracted from the datasheets of the Saint-Gobain BC-400 plastic scintillator and of the BCF-92 WLS fibers: in table I the main parameters are shown.

TABLE I. – *Optical properties of the scintillator tiles and the WLS fibers.*

Model	Material	Refractive index	Emission peak	Light yield (per keV)	Attenuation length
BC-400	Polyvinyltoluene	1.58	423 nm	$\sim$ 10 photons	160 cm
BCF-92 (core)	Polystyrene	1.60	492 nm	N/A	> 3.5 m
BCF-92 (cladding 1)	Acrylic	1.49	N/A	N/A	N/A
BCF-92 (cladding 2)	Fluor-acrylic	1.42	N/A	N/A	N/A

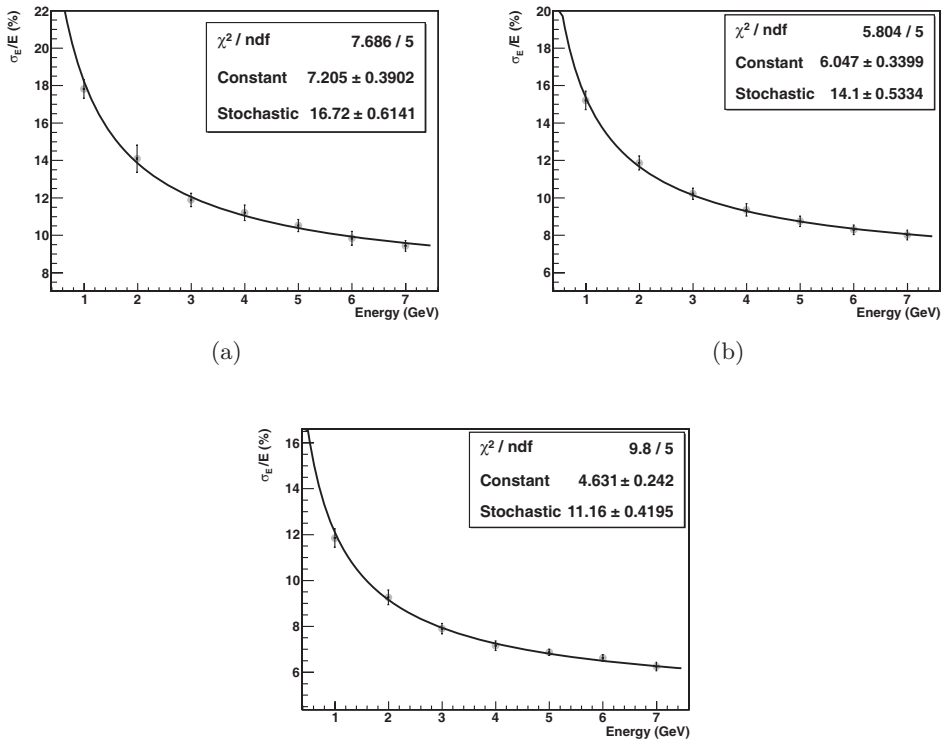

Fig. 4. – Energy resolution obtained with the optical simulation with a reflection coefficient of 0.2 (a), 0.4 (b) and 0.6 (c).

While the propagation of the light from the plastic scintillator to the WLS fibers is handled by the Geant4 program using the rules of the geometric optics (reflection and refraction), particular attention must be paid for the definition of the scintillator-lead interface. As stated in sect. **1**, no reflective material has been inserted between the scintillator and lead tiles. However, the reflectivity of the interface cannot be set to zero for the following reasons:

– the presence of a tiny air gap between the tiles (due to mechanical imperfections) which makes total internal reflection phenomena at certain angles possible;

– the presence of a partially reflective zinc coating on the surface of the lead tiles.

For these reasons the internal borders of the scintillator tiles have been defined as a "LogicalSkinSurface", to which a reflection coefficient has been associated, defined as a photon reflection probability between 0 and 1. The number of photons collected by each fiber is counted by a sensitive detector placed at the end of each fiber; the fibers are then grouped in bundles of nine each as in the experimental case. A histogram is filled with the total number of photons collected in each event by all the fibers and fitted with a Gaussian function to extract the resolution parameter.

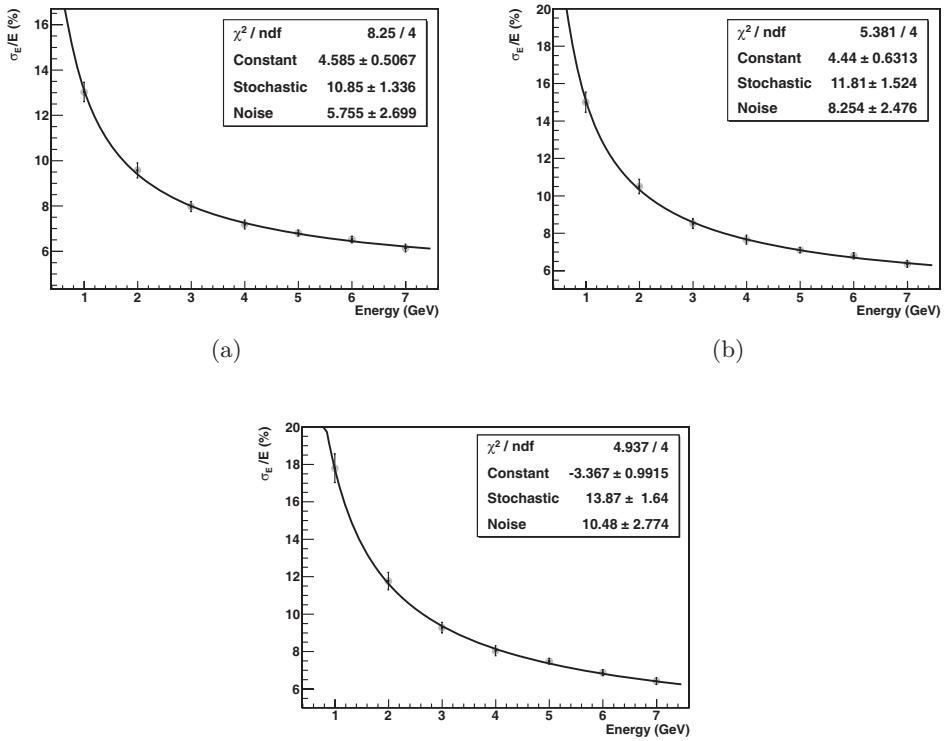

Fig. 5. – Energy resolution obtained with the optical simulation with a reflection coefficient of 0.6 and various noise values (40 (a), 80 (b) and 120 (c) photons).

As will be shown, the energy resolution of the calorimeter depends strongly on the reflection coefficient used for the LogicalSkinSurface, so many tests have been performed to find the coefficient which better fits to the data. An example of the energy resolution obtained with various values of the reflection coefficient (0.2, 0.4 and 0.6) is shown in fig. 4.

As can be seen, the energy resolution improves with the reflection coefficient, hence increasing the light collection efficiency; this behaviour is somehow expected, and is the reason why the scintillator tiles of the sampling calorimeters are usually wrapped by a reflective coating material. The energy resolution is deeply different from the values obtained in the preliminary simulation, with stochastic terms of 18.7, 14.1 and 11.2% for reflection coefficients of 0.2, 0.4 and 0.6, respectively. Also the constant term depends on the reflection coefficient, varying from 7.2% with a 0.2 value to 4.6% in the 0.6 case.

To take into account also the noise contribution, a noise term is introduced in the off-line analysis adding, for each readout channel, a constant number of photons multiplied by a random value uniformly distributed between -1 and 1. The energy resolution has then been fitted with the function $\frac{\sigma_E}{E} = P_0 \oplus \frac{P_1}{\sqrt{E}} \oplus \frac{P_2}{E}$: the P_2 term takes into account the noise effects and dominates the energy resolution at low energies, because of the $\frac{1}{E}$ dependence. The results obtained in terms of energy resolution for different values of noise are shown in fig. 5.

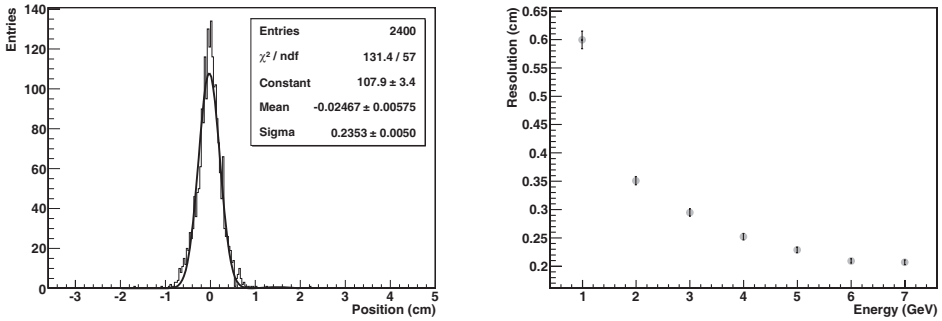

(a) (b)

Fig. 6. – (a) Residuals for a 4 GeV simulated electron beam and (b) obtained spatial resolutions at various energies.

As can be seen, the introduction of the noise term modifies the energy resolution behaviour at low energies, with a fitted noise term which depends on the amount of photons added in the analysis. The best agreement between data and simulation has been obtained using a reflection coefficient equal to 0.62 and a noise term of 130 photons (which correspond to the signal produced by 1.5 MIPs in the central channels of the calorimeter); a comparison between data and simulation is presented in sect. **4**.

Knowing the number of photons collected by each fiber and using the fact that the calorimeter has a segmented readout in the x-y direction, it is possible to reconstruct the hit position evaluating the calorimeter spatial resolution. The position reconstruction is based on the logarithmic barycenter algorithm described in [12]; the output channels, indicated in fig. 1(b), have been divided in x and y planes according to the following

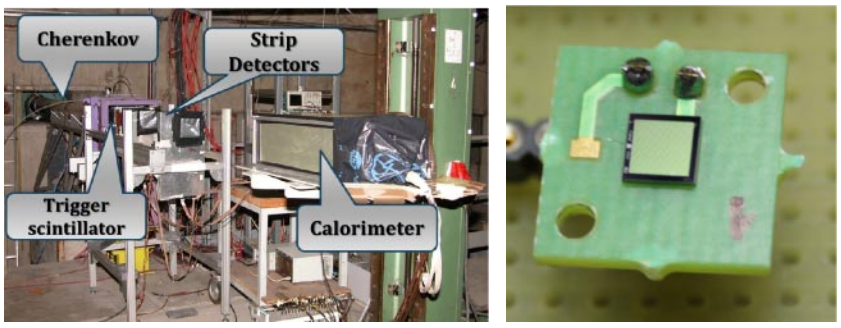

(a) (b)

Fig. 7. – (a) The experimental setup at the PS T9 beamline and (b) a picture of the 9 mm^2 SiPM bonded on the PCB.

TABLE II. – *FBK-irst SiPM specifications: the breakdown voltage is an indicative value.*

Number of pixels	Spectral response range [17]	Breakdown voltage	Time resolution [17]	Gain [18]	PDE [17] (500 nm)
3600	380–810 nm	~ 31 V	165 ps	$\sim 10^6$	$\sim 35\%$

relations:

$$
\begin{aligned}
Layer_{1X} &= ([1]+[5]+[9]+[13]), & Layer_{1Y} &= ([1]+[2]+[3]+[4]),\\
Layer_{2X} &= ([2]+[6]+[10]+[14]), & Layer_{2Y} &= ([5]+[6]+[7]+[8]),\\
Layer_{3X} &= ([3]+[7]+[11]+[15]), & Layer_{3Y} &= ([9]+[10]+[11]+[12]),\\
Layer_{4X} &= ([4]+[8]+[12]+[16]), & Layer_{4Y} &= ([13]+[14]+[15]+[16]).
\end{aligned}
$$

To estimate the coordinate of the incident particle, the center of gravity has been calculated using the following equations:

$$
X_{calc} = \frac{\sum_i w_i x_i}{\sum_i w_i}, \qquad w_i = Max\left\{0, \left[w_0 + \ln\frac{E_i}{E_{tot}}\right]\right\}, \tag{1}
$$

where the x_i are the x or y coordinates of the center of the planes, w_i are weight factors, E_i is the number of photons deposited in each plane and E_{tot} is the total number of photons. The w_0 parameter is free and dimensionless and has a twofold task: the definition of a threshold for the inclusion of a plane in the coordinate calculation and of the relative importance of the tails of the shower. The spatial resolution has been computed using the residuals, that is the difference between the impact point of the particle on the calorimeter (extracted from the simulation) and the position reconstructed with the center of gravity method; the w_0 value has been chosen in order to minimize the residuals. The results are presented in fig. 6.

The resolution is of the order of ~ 6 mm at 1 GeV, it improves with the energy of the primary particle and it approaches an asymptote (~ 2 mm) at high energy, due to the finite readout pitch of the calorimeter. Better results can be, in principle, obtained increasing the numbers of readout channels, thus reducing the readout pitch.

3. – The experimental setup

The shashlik calorimeter has been tested at the CERN PS-T9 [13] beamline in October 2009 with negative particles in a momentum range between 1 and 7 GeV/c. The setup is composed of two Cherenkov detectors for the electron tagging, two silicon strip chambers for the track reconstruction and a 10×10 cm^2 plastic scintillator for the trigger. A picture of the experimental setup is shown in fig. 7(a).

Each silicon chamber consists of a pair of single-sided silicon strip detectors (9.5×9.5 cm^2 with a thickness of 410 μm) with a readout pitch of 242 μm, one floating strip and a spatial resolution of the order of 30 μm [14].

The optical readout of the calorimeter was performed using 16 squared SiPMs with a sensitive area of 9 mm^2. SiPMs are multipixel passively quenched silicon photodiodes operated in Geiger-Muller (GM) avalanche mode: each pixel can be considered as a diode

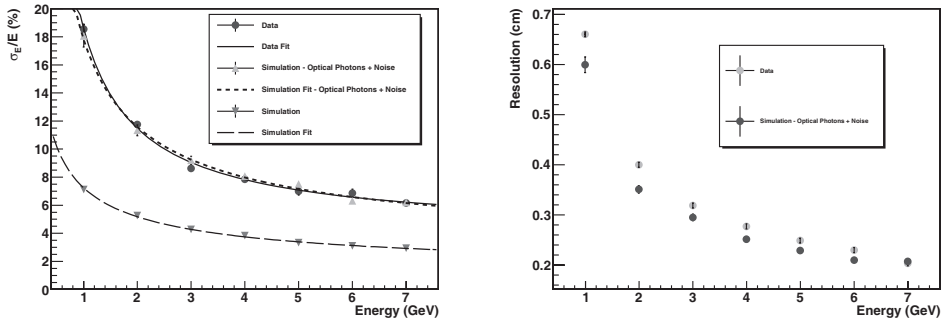

(a) (b)

Fig. 8. – Comparison of the energy resolution (a) and spatial resolution (b) obtained with the data and with the Geant4 simulations using a reflection coefficient of 0.62.

reverse-biased over its breakdown voltage which gives a digital information when hit by a photon. The analog response to a moderate flux of photons is obtained considering the number of fired pixels. More information on the SiPMs operating principles can be found in [15, 7]. The SiPMs used in the tests are manufactured by FBK-irst [16], which is involved in an R&D project with INFN in the framework of the FACTOR (Fiber Apparatus for Calorimetry and Tracking with Optoelectronic Read-out) collaboration. The main characteristics of the SiPMs used in the tests are shown in table II, while a picture of the device is presented in fig. 7(b).

The output signal of the SiPMs is delayed by ~ 140 ns (to synchronize it with the data acquisition) and then sampled by a CAEN V792 12 bit QDC. In order to equalize the power consumption the SiPMs are biased in groups of four using two different power supplies: their bias voltages and current consumption were monitored at the end of each run.

4. – Data/simulation comparison

The first event selection is performed using the information provided by the silicon strip chambers, selecting only the single-track events, while the electron events are selected using the Cherenkov detector information. The output channels of the calorimeter are then summed to extract the total energy deposit after an equalization procedure using a MIP beam impinging on the calorimeter. The total energy deposit is then fitted with a Gaussian function to extract the resolution parameter. To compute the spatial resolution, the readout channels have been divided in planes as explained in sect. **2** to use the reconstruction algorithm described in [12]. A comparison of the results obtained in terms of energy and spatial resolution between the simulated and real data is presented in fig. 8 and table III.

TABLE III. – *Energy resolution parameters obtained with the Geant4 simulations and data run.*

	Simulation	Optical Simulation	SiPMs
Constant	$1.19 \pm 0.1\%$	$2.76 \pm 1.17\%$	$3.97 \pm 0.64\%$
Stochastic	$7.05 \pm 0.08\%$	$13.99 \pm 1.59\%$	$11.48 \pm 1.27\%$
Noise	N.A.	$10.7 \pm 2.72\%$	$14.14 \pm 1.18\%$

For what concerns the energy resolution, a good agreement has been obtained between data and optical simulation. Given that the resolution parameters extracted from the simulation fit are slightly different from the ones obtained in the data, the off-line analysis and the treatment of the noise contribution have to be refined. Also for the spatial resolution the agreement between the data and the optical simulation is quite good, even if some discrepancies can be seen at low energies: these effects may originate from small non-uniformities between the SiPM which become negligible by increasing the energy because of the increased number of produced photons.

5. – Conclusions

A Geant4 simulation including the optical processes has been developed to describe a shashlik calorimeter with a SiPM readout. The obtained results have shown that the absence of a reflective coating between the scintillator and lead tiles (and the resulting small reflection coefficient) limits the calorimeter performances in terms of energy resolution. A good agreement between data and optical simulation can be obtained using a reflection coefficient of 0.62. For this reason, some hardware modifications have to be done in order to improve the light collection of the calorimeter, for example the scintillator tiles wrapping with a reflective material and the insertion of mirrors on the opposite readout ends of the WLS fibers. A new beamtest is foreseen in summer 2011 at CERN to test the improved version of the calorimeter using both a low-energy (1–7 GeV) electron beam and a high-energy (up to 120 GeV) tagged photon beam.

* * *

The author is grateful to: the Insulab group of the Insubria University (in particular M. Prest) and the Trieste INFN section (in particular E. Vallazza) for the effort and the support to this work; the mechanical workshop of the Trieste INFN section for its contribution in the calorimeter assembly.

REFERENCES

[1] Fessler H. *et al.*, *Nucl. Instrum. Methods Phys. Res. A*, **228** (1985) 303.
[2] Dzhelyadin R., *Nucl. Instrum. Methods Phys. Res. A*, **581** (2007) 384.
[3] Alvsvaag S. J. *et al.*, *Nucl. Instrum. Methods Phys. Res. A*, **425** (1999) 106.
[4] Abreu P. *et al.*, *Nucl. Instrum. Methods Phys. Res. A*, **378** (1996) 97.
[5] Atoian G. S. *et al.*, *Nucl. Instrum. Methods Phys. Res. A*, **531** (2004) 467.
[6] Benvenuti A. C. *et al.*, *Nucl. Instrum. Methods Phys. Res. A*, **432** (1999) 232.
[7] Dolgoshein B. *et al.*, *Nucl. Instrum. Methods Phys. Res. A*, **442** (2000) 187.
[8] Allison J. *et al.*, *Nucl. Instrum. Methods Phys. Res. A*, **506** (2003) 250.
[9] Saint-Gobain scintillating optical fibers datasheet, `http://www.detectors.saint-gobain.com/uploadedFiles/SGdetectors/Documents/Brochures/Scintillating-Optical-Fibers-Brochure.pdf`.
[10] Recommended Geant4 physics list can be found at `http://geant4.cern.ch/support/proc_mod_catalog/physics_lists/referencePL.shtml`.
[11] Fabjan C. W. and Gianotti F., *Rev. Mod. Phys.*, **75** (2003) 1243.
[12] Awes T. C. *et al.*, *Nucl. Instrum. Methods Phys. Res. A*, **311** (1992) 130.
[13] Durieu L., Martini M. and Müller A. S., "Optics studies for the T9 beam line in the CERN PS East Area secondary beam facility", in *Proceedings of the 19th IEEE PAC2001, CERN-PS-2001-037-AE.*
[14] Prest M. *et al.*, *Nucl. Instrum. Methods Phys. Res. A*, **501** (2003) 280.

[15] Piemonte C., *Nucl. Instrum. Methods Phys. Res. A*, **568** (2006) 224.
[16] FBK-irst internet page: `http://www.itc.it/irst/`.
[17] Collazzuol G. *et al.*, *Nucl. Instrum. Methods Phys. Res. A*, **581** (2007) 461.
[18] Piemonte C. *et al.*, "Recent developments on Silicon Photomultipliers produced at FBK-irst", *2007 IEEE Nuclear Science Symposium Conference Record*, paper N41-2, pp. 2089–2092.